Cladosporol A Stimulates G1-Phase Arrest of the Cell Cycle by Up-Regulation of p21$^{waf1/cip1}$ Expression in Human Colon Carcinoma HT-29 Cells

Diana Zurlo,[1] Cinzia Leone,[1] Gemma Assante,[2] Salvatore Salzano,[3] Giovanni Renzone,[4] Andrea Scaloni,[4] Caterina Foresta,[1] Vittorio Colantuoni,[1,5] and Angelo Lupo[1,5]*

[1]*Dipartimento di Scienze Biologiche ed Ambientali, Facoltà di Scienze, Università del Sannio, Benevento, Italy*
[2]*Dipartimento di Patologia Vegetale Università degli Studi di Milano, Milano, Italy*
[3]*CNR Istituto di Endocrinologia ed Oncologia Sperimentale "G. Salvatore", Università Federico II, Napoli, Italy*
[4]*Laboratorio di Proteomica e Spettrometria di Massa, ISPAAM, Consiglio Nazionale delle Ricerche, Napoli, Italy*
[5]*Dipartimento di Biochimica e Biotecnologie Mediche Università Federico II, Napoli, Italy*

Cladosporols, purified and characterized as secondary metabolites from *Cladosporium tenuissimum*, display an antifungal activity. In this study, we tested the antiproliferative properties of cladosporol A, the main isoform of this metabolite family, against human cancer cell lines. By assessing cell viability, we found that cladosporol A inhibits the growth of various human colon cancers derived cell lines (HT-29, SW480, and CaCo-2) in a time- and concentration-dependent manner, specifically of HT-29 cells. The reduced cell proliferation was due to a G1-phase arrest, as assessed by fluorescence activated cell sorting analysis on synchronized HT-29 cells, and was associated with an early and robust over-expression of p21$^{waf1/cip1}$, the well-known cyclin-dependent kinases inhibitor. This suggests that the drug may play a role in the control of cancer cell proliferation. Consistently, cyclin D1, cyclin E, CDK2, and CDK4 proteins were reduced and histone H1-associated CDK2 kinase activity inhibited. In addition to p21$^{waf1/cip1}$, exposure to 20 μM cladosporol A caused a simultaneous increase of pERK and pJNK, suggesting that this drug activates a circuit that integrates cell cycle regulation and the signaling pathways both involved in the inhibition of cell proliferation. Finally, we showed that the increase of p21$^{waf1/cip1}$ expression was generated by a Sp1-dependent p53-independent stimulation of its gene transcription as mutagenesis of the Sp1 binding sites located in the *p21* proximal promoter abolished induction. To our knowledge, this is the first report showing that cladosporol A inhibits colon cancer cell proliferation by modulating p21$^{waf1/cip1}$ expression. © 2011 Wiley Periodicals, Inc.

Key words: cladosporol A; cell cycle; G1 phase arrest; p21$^{waf1/cip1}$; transcription

INTRODUCTION

Chemoprevention consists in the administration of natural and/or synthetic compounds to prevent the occurrence of degenerative diseases and, more recently, various cancer types. Vitamins, minerals, carotenoids, flavonoids, organsulfurs, isothiocyanates, indoles, monoterpenes, phenolic acids, and chlorophylls, are all included in the list of natural and already available compounds able to interfere with the various steps of the carcinogenetic process through different mechanisms and distinctive molecules [1–3]. Isolation and characterization of new natural molecules from plants, fungi, and microrganisms will increase the number of these therapeutic tools to inhibit cancer cells proliferation.

Cladosporols are secondary metabolites purified from *Cladosporium tenuissimum*, strain ITT21, cultured in sugar-rich media [4]. This fungus is a hyperparasite of rust fungi and its derived compounds possess antifungal activity [5]. The main metabolite was isolated as a white powder, representing more than 30% of the crude extract (Figure 1A). Its spectral analyses were consistent with a $C_{20}H_{16}O_6$ molecular formula and a dimeric decaketide binaphthyl structure [6]. Cladosporols were initially characterized as plant regulators,

Abbreviations: CRC, colorectal cancer; CDK, cyclin-dependent kinase; CDKI, cyclin-dependent kinase inhibitor; ERK, extracellular signal-regulated protein kinase; JNK, c-Jun NH2-terminal kinase; PCNA, proliferating cell nuclear antigen; RB, retinoblastoma; D-MEM, Dulbecco's Modified Eagle's Medium; FBS, fetal bovine serum; RT-PCR, reverse transcriptase-polymerase chain reaction; GAPDH, glyceraldehyde-3-phosphate dehydrogenase; MAPKs, mitogen-activated protein kinases; MS, mass spectrometry.

*Correspondence to: Dipartimento di Scienze Biologiche ed Ambientali, Facoltà di Scienze, Università del Sannio, via Port'Arsa 11, 82100 Benevento, Italy.

Received 10 January 2011; Revised 2 September 2011; Accepted 19 September 2011

DOI 10.1002/mc.20872

Published online in Wiley Online Library (wileyonlinelibrary.com).

© 2011 WILEY PERIODICALS, INC.

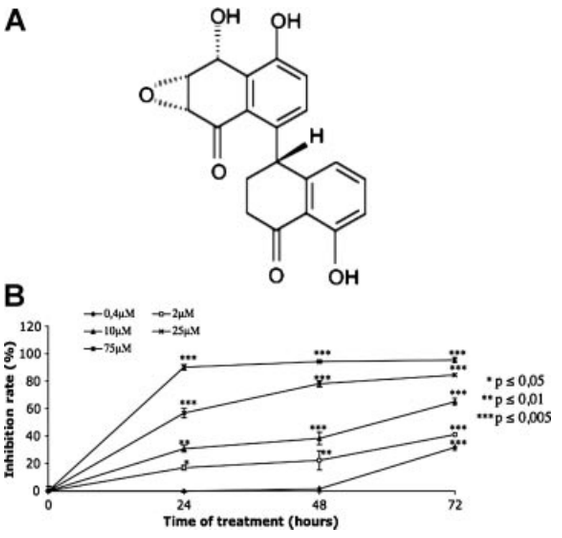

Figure 1. (A) Chemical structure of cladosporol A. (B) Dose-dependent cytotoxicity of cladosporol A on HT-29 cells, as determined by the CellTiter Aqueous One Cell Proliferation Assay. Cells were seeded in 96-well plates in order to reach the density of 10^6 cells/cm^2 in standard conditions (10% charcoal/dextran-treated FBS containing 1% penicillin–streptomycin and 1% L-glutamine). After 24 h, increasing concentrations of cladosporol A (from 0.4 to 75 µM) were used to stimulate cells and the growth was evaluated up to 72 h through measurement of absorbance at 490 nm. Results were expressed as the optical density ratio of the difference between the control and the treated cells to the control cells. Each point was done in triplicate and the experiment was repeated two times.

then as inducers of hyphal malformations in *Phytophthora capsici* and, lastly, as inhibitors of β-1, 3-glucan synthetase, the enzyme responsible for the synthesis of the fungal cell wall components [7,8]. Cladosporols are able to inhibit almost completely spore germination in a great number of rust fungi, such as *Uromyces appendiculatus*, *Melampsora pinitorqua*, *Cronartium flaccidum*, and provoke the reduction of radial growth of non-rust fungi as in colonies of the phytopathogenic fungi like *Alternaria alternata*, *Botrytis cinerea*, *Cercospora beticola*, among the Oomycota, *Phytophthora capsici*, *P. cinnamomi*, *P. erytroseptica* and among human pathogenic strains of *Candida* sp. The antifungal activity of cladosporols likely resides in the intrinsic toxicity of the 2-tetralone chromophore and in highly reactive functionalities, such as the epoxy-alcohol moiety, very similar to (+)-isoepoxidon, also reported as a β-1, 3-glucan biosynthesis inhibitor, or other similar compounds [9–11]. These bioactive molecules strongly influence the pathogenicity of *C. tenuissimum* and play a major role in its hyperparasitism.

Colorectal cancer (CRC) is one of the most widespread tumors in Western countries. The most recent statistics confirm that only in the USA about 146,970 new cases of CRCs will be diagnosed in the next year and 49,920 patients will die of this disease [12]. In addition to genetic alterations in tumor suppressor genes, such as *P53* and adenomatous polyposis coli (*APC*), loss of cell cycle control, increased cell survival signaling and inhibition of apoptosis are the most common events observed in CRC promotion and/or progression [13–15].

For these reasons, new molecules affecting the cell cycle might be helpful tools to prevent the earliest events in carcinogenesis [16,17]. Cell cycle progression is modulated by cyclins and cyclin-dependent kinases (CDKs) interactions [18]. These protein complexes are sequentially activated during the cell cycle allowing the transition through the G1, S, and G2/M phases [19]. Under different conditions, the cyclin-CDK complexes are inhibited by the binding of CDK inhibitors (CDKIs), two main groups of which have been identified and characterized so far, the CIP/KIP and INK4 families [20,21]. $p21^{waf1/cip1}$ is one of the most important members of the CIP/KIP family, is recognized as a fundamental player in the control of cell proliferation [22,23] and identified as the target of the p53-dependent growth-arrest after DNA-damage induction in various cell types [24,25]. Indeed, $p21^{waf1/cip1}$ expression is modulated through p53-dependent and -independent mechanisms [26,27]. The majority of human cancers bear mutated forms of p53 and, therefore, it is interesting to investigate p53-independent but p21-mediated mechanisms of cell cycle regulation. Novel findings on this topic might suggest new potential intervention in managing human cancers.

Epidemiologic studies demonstrated a tight correlation between CRC diffusion and red meat, fatty acids, and alcohol intake [28]. Moreover, a dramatic difference in CRC incidence has been observed among populations of different ethnic groups that may be ascribable to the different dietary regimens followed in the different countries [29]. Thus, CRC frequency in Europe and USA (where the consumption of fat and red meat in the diet is very high) is higher than that observed in Asia (where people are used to eating large amounts of vegetables). Consumption of high amounts of fruit and vegetables may result in a reduction of CRC occurrence and, therefore, a chemopreventive approach could be a productive strategy to control the disease diffusion [30–32].

Along this reasoning, Chen et al. [33] have recently demonstrated that the growth of the human gastric carcinoma derived cells (MGC-803) is inhibited by cladosporol isolated from the paclitaxel-producing strain *Alternaria alternata* var: *monosporus*. Here, we tested the antiproliferative properties of cladosporol A on three CRC derived cell lines (HT-29, SW480, and CaCo-2) to elucidate the underlying molecular mechanisms. In particular, we show that exposure of HT-29 cells to the drug causes a p21-dependent, p53-independent

cell cycle arrest at the G1/S phase. This effect is accompanied by a robust $p21^{waf1/cip1}$ overexpression, a significant CDK2, CDK4, cyclin D1, and cyclin E protein down-regulation and a CDK2 kinase activity inhibition. Moreover, we provide the first evidence that extracellular signal-regulated protein kinase (ERK) [and c-Jun NH2-terminal kinase (JNK) also] might function as mediator of the cladosporol A-induced redox response and inhibition of HT-29 cell growth. Finally, our findings demonstrate that cladosporol A-mediated impairment of CRC cell survival is due to an Sp1-modulated increase of $p21^{waf1/cip1}$ gene transcription.

MATERIALS AND METHODS

Cells, Antibodies, and Reagents

HT-29, SW480, CaCo-2, and HCT116 (from human colon cancers) cells were obtained from the American Type Culture Collection (Rockville, MD). These cell lines bear different genetic abnormalities typical of human CRC, because they have truncated or mutant APC gene. Moreover, SW480 cells express both P53 (Arg273 > His and Pro309 > Ser) and RAS (Val12 > Glu) mutated forms. HT-29 cells bear a mutated *p53* (Arg 273 > His), but a wild-type *ras* allele. HCT116 cells carry a mutated form of RAS and a wild-type P53. HCT116 p53−/− were a kind gift from Dr. Bevilacqua (University of Naples ''Federico II''). Finally, CaCo-2 cells express wild-type *RAS*, but carry a mutated *p53* allele form [34].

Antibodies against $p21^{waf1/cip1}$, cyclin E, D1, A and B1, CDK2, CDK4, Cdc2p34, proliferating cell nuclear antigen (PCNA), pERK, pJNK, p53, retinoblastoma (RB), and β-actin were purchased from Santa Cruz Biotechnology (Santa Cruz, CA). Anti-mouse and anti-rabbit IgG peroxidase-linked secondary antibodies, A/G plus agarose beads, ECL and ECL Plus Western blotting detection kit were purchased from Amersham Life Science (Little Chalfont, England). Dulbecco's Modified Eagle's Medium (D-MEM), RPMI1640, D-luciferin sodium salt, trichloroacetic acid, propidium iodide (PI), thiazolinedione, apocynin, UO126 and PD98059 were from Sigma (St.Louis, MO). Fetal bovine serum (FBS), penicillin–streptomycin, L-glutamine, trypsin-EDTA, and OptiMEM I were obtained from Gibco (Carlsbad, CA). Charcoal/dextran-treated FBS was purchased from Hyclone (Logan, Utah). Fetal calf serum, Lipofectamine 2000, TRIZOL, SuperScript II reverse transcriptase were from Invitrogen (Carlsbad, CA). The CellTiter Aqueous One Cell Proliferation Assay was obtained from Promega (Madison, WI). SYBR Green and Ready Strip IPG strips were purchased from BioRad (Hercules, CA). AmpliTaq Gold was purchased from Applied Biosystems (Foster City, CA).

Cell Culture and Cladosporol A Treatment

Human colon adenocarcinoma cell lines HT-29, Caco-2, and SW480 were grown as a monolayer in D-MEM containing 10% FBS, 1% penicillin–streptomycin, and 1% L-glutamine. HCT116 were grown in RPMI1640 medium containing 10% FBS, 1% penicillin–streptomycin and 1% L-glutamine. All the cells were cultured in 100 mm plates, at 70–80% confluence, in a 5% CO_2 humidified atmosphere, at 37°C.

Cladosporol A treatments were carried out in presence of 10% charcoal/dextran-treated FBS containing 1% penicillin–streptomycin and 1% L-glutamine, whereas the cells were maintained at 40% confluence. Cladosporol A was dissolved in dimethylsulfoxide (DMSO) and mixed with fresh medium to achieve the final concentration. In all treatments, the DMSO final concentration in the medium was <0.1%. In separate experiments, cells were treated with increasing concentrations of cladosporol A, for the indicated times. We also performed the same experiments by culturing the cells in D-MEM (or RPMI1640) containing 10% FBS and the results obtained were identical.

Cell Viability and Lipid Peroxidation Assays

The growth rate of HT-29 cells was evaluated using the CellTiter Aqueous One Cell Proliferation Assay (Promega, Madison, WI), following the manufacturer's procedure. Cells were seeded in 96-well plates in order to reach the density of 10^6 cells/cm^2 in standard conditions (10% FBS). After 24 h, increasing concentrations of cladosporol (from 0.4 to 75 μM) were added to stimulate cells and the growth was evaluated from 24 up to 72 h. The inhibition rate was expressed as the optical density ratio of the difference between the control and the treated cells to the control. The concentration of cladosporol A required for 50% reduction in cell survival (IC_{50}) was calculated using standard curves. Each time point was done in triplicate and the experiment repeated at least two times. The absorbance at 490 nm was measured on a microplate reader (BenchMark, Bio-Rad, Hercules, CA).

To further evaluate cell growth after treatment with cladosporol A, cells were plated in 12-well plates at density of 10^6 cells/cm^2. After treatment, the cells were washed with PBS, trypsinized and collected in culture medium. Cell counting was performed by means of a Bürker's hemocytometer. Three counts for each well were made and the mean value and the standard deviation were calculated.

Lipid peroxidation products from cells were measured by the thiobarbituric acid colorimetric assay. Briefly, an aliquot of the lysate (100 μl) was added to 200 μl of 10% (w/v) trichloroacetic acid and, after centrifugation at 3,000 rpm for 10 min, 260 μl of 0.5% (w/v) thiobarbituric acid were

added and the mixture was heated at 80–100°C for 30 min. After cooling, malondialdehyde (MDA) formation was recorded by spectrophotometry at 550 nm, in a microplate reader spectrophotometer (Bio-Rad). The results are presented as micromoles of MDA/μg of cell protein determined by the Bio-Rad protein assay. A standard curve of MDA was used to quantify the MDA levels formed during the experiments.

Flow Cytometry Analysis

HT-29 cells were plated at similar confluency, as described above, and after 24 h, synchronized by a 48 h serum deprivation in 0.1% FBS. An aliquot of the cells was stimulated with 5, 10, or 20 μM cladosporol A for different times (4, 8, 12, 24, and 48 h) in the presence of D-MEM containing 10% FBS. Another aliquot of cells was allowed to grow again in the complete medium; these samples were used as control. Afterwards, 2 millions of whole floating and adherent cells of each sample were collected, washed in cold calcium and magnesium-free phosphate buffered saline (PBS), fixed and permeabilized in 70% cold ethanol for 30 min. Ethanol was removed by washing with PBS and cells were incubated in PBS containing 10 μg/ml deoxyribonuclease-free ribonuclease, for 10 min, at 4°C. Finally, 50 μg/ml PI was added and the cells were incubated at 4°C, overnight, in a dark room. Cells were analyzed by flow cytometry using a FACScan Flow Cytometer Apparatus 488 nm argon-laser (Becton Dickinson, Mountain View, CA). Analysis of the results was performed with CellFit DNA software (version 2.01.2 Becton Dickinson) run on HP series 9000 workstation Apollo OS Consort32 (Hewlett-Packard, Palo-Alto, CA). Width gating was performed to exclude doublets from G2/M region on dot-plot. For each sample, 2,000 events were stored in list mode. The same experiment was performed also using p53+/+ and p53−/− HCT116 cells.

Western Blotting Analysis and Kinase Assay

Treated and untreated cells were lysed in Ripa buffer (150 mM NaCl, 50 mM Tris–HCl, pH 7.6, 10 mM EDTA, 1% NP-40) containing also protease inhibitors cocktail and then centrifugated at 13,000 rpm for 10 min, at 4°C. Supernatant containing total proteins was quantified and 80 μg of each sample were separated on 12% SDS–PAGE and transferred onto a PVDF membrane (Millipore, Bedford, MA) by electroblotting. Membranes were blocked in 5% non-fat dry milk and probed with specific antibodies at 4°C, overnight. After a 1-h incubation with IgG-peroxidase-linked antibody, at room temperature, signals were detected by chemiluminescence with ECL or ECL Plus reagents. The relative intensity of protein bands was measured using the Molecular Imager Chemi-Doc imaging system (Bio-Rad) and evaluated by the Quantity One software (Bio-Rad).

To determine the histone H1-associated CDK2 kinase activity, 200 μg of protein lysates from each sample was precleared with protein A/G plus agarose beads and CDK2 was immunoprecipitated using a specific anti-CDK2 antibody (2 μg) and protein A/G plus agarose beads. The beads were washed three times with lysis buffer and finally twice with kinase assay buffer. Phosphorylation of histone H1 was measured by incubating the beads with 30 μg of ''hot'' kinase solution (4 μg of histone H1, 1 μl of γ-^{32}P-ATP, 0.5 μl of 0.1 mM of ATP and 24.5 μl of kinase buffer) for 1 h at 37°C. The reaction was stopped by boiling the samples in SDS sample buffer for 5 min. The samples were analyzed by 12% SDS–PAGE and the gel was dried and subjected to autoradiography.

Reverse Transcription-PCR (RT-PCR) and Real-Time Quantitative PCR (RT-qPCR) Assays

RNA was isolated from treated and untreated HT-29 cells using TRIZOL reagent according to the manufacturer's instructions. The purity, integrity, and concentration of total RNA were determined by gel electrophoresis and UV spectroscopy. To obtain the cDNAs, 2 μg of total RNA were reverse transcribed using SuperScript™ II reverse transcriptase. For each sample, total RNA was incubated with 2.5 μM random primers at 70°C, for 10 min. After this step, a mixture containing 0.5 mM dNTP, 10 mM DTT, 5 U of SuperScript™II enzyme (Invitrogen, Carlsbad, CA) and First Strand buffer was added to the sample, which was incubated for 10 min, at room temperature. Subsequently, the reaction proceeded at 42°C, for 50 min and, finally, was stopped by incubation at 70°C, for 15 min. PCR analysis was performed for $p21^{waf1/cip1}$ gene (351 bp amplicon) by using the following primers: 5′-GCGATGGAACTTCGACTTTGT-3′ and 3′-GGGCTTCCTCTTGGAGAAGAT-5′. As an internal control for the densitometric analysis of the amplified fragments, the housekeeping human glyceraldehyde-3-phosphate dehydrogenase (GAPDH) gene (400 bp amplicon) was utilized by using the following primers: 5′-GACCCCTTCATTGACCTCAACTACATG-3′ and 3′-GTGCACCACCCTGTTGCTGTA GCC-5′. PCR reaction was performed by adding to each sample a 20 μl mixture containing 2 μl of the newly synthesized cDNA, PCR Buffer II, 1.5 mM $MgCl_2$, 0.2 mM dNTP, 0.2 μM primers, and 2.5 U of *AmpliTaq®Gold* (Applied Biosystem, Foster City, CA). DNA amplification was carried out allowing 30 and 35 PCR cycles of reactions (94°C for 1 min, 58°C for 30 s, 72°C for 1 min, for each cycle). PCR products were analyzed on 1.2% agarose gels containing ethidium bromide. Gel images were acquired with the Chemi-Doc imaging system (Bio-Rad).

For RT-qPCR, a 20 μl mixture containing 1 μg of cDNA, 10 μl of SYBR Green and 0.4 μM primers of $p21^{WAF1/Cip1}$ or GAPDH was added to each sample. Thirty-five amplification cycles were performed according to the program used in RT-qPCR assay. For each sample, analysis was carried out in triplicate and the results were evaluated by the Gene Expression Relative Quantitation program (Bio-Rad).

Plasmids and Transient Transfection Experiments

The human wild-type $p21^{waf1/cip1}$ promoter-luciferase fusion construct (pWWP) and the mutants pWP124, pWP101, pWP101-mtSp1-3, pWP101-mtSp1-4, pWP101-mtSp1-5/6 were a generous gift from Dr. Y. Sowa (Department of Molecular-Targeting Cancer Prevention, Kyoto Prefectural University of Medicine, Kyoto, Japan) [35,36]. As an internal transfection control, we used the RSV-βGal plasmid, expressing β-galactosidase cDNA driven by the strong Rous Sarcoma Virus (RSV) promoter.

The day before transient transfection, HT-29 cells were plated in 12-well plates to reach a 70% confluence. After 24 h, growth medium was replaced with OPTI-MEM®I, (Gibgo, Carlsbad, CA) without serum and antibiotics, and cells were transfected using lipofectamine 2000 reagent according to manufacturer's instructions. About 10–12 h after transfection, cells were washed and treated with 20 μM cladosporol A. Transfection samples were carried out in triplicate and the transactivation activities were evaluated by luciferase assay. The achieved values were normalized by β-galactosidase assay and the average value for each triplicate was calculated.

Bi-Dimensional Electrophoresis

HT-29 cells were plated at 40% confluence and treated or not with 20 μM cladosporol A for 8 h. Treated and untreated cells were collected into a buffer containing 8 M urea, 4% CHAPS, 40 mM Tris, 65 mM DTT and Protease Inhibitors cocktail, and lysed by three cycles of sonication at 70% amplitude. After centrifugation at 13,000 rpm for 30 min, at 4°C, total proteins were extracted and quantified by spectroscopy at 595 nm. For each sample, 200 μg of total proteins were solubilized in a buffer with 8 M urea, 2% CHAPS, 100 mM DTT, 0.5% ampholytes, and analyzed. For isoelectrofocusing, 7 cm strips with a 4–7 pH range were used; strip rehydration proceeded for 16 h. The focusing system was the IPG (GE Healthcare, Chalfont St. Giles, UK) and the program was set at an increasing voltage until 1,000 V for 1 h and then until 5,000 V for 160 min, at 20°C. Afterwards, the strips were equilibrated in 50 mM Tris–HCl, pH 8.8, 2% SDS, 7 M urea, 10% glycerol, 2% DTT, for 15 min, and then incubated in 50 mM Tris–HCl, pH 8.8, 2% SDS, 7 M urea, 10% glycerol, 2.5% iodoacetamide, bromophenol blue, for 15 min. Each strip was accommodated onto a 12% polyacrylamide gel and the proteins were separated at 120 V, for 3 h. Gels were fixed in 7% acetic acid, 50% methanol, for 15 min, and stained with Gel Code Blue Stain reagent (Pierce, Thermo Fisher Scientific, Rockford, IL). Gels were scanned with a GS-800 calibrated densitometer (Bio-Rad) and analyzed by using the PD Quest v.6 software. The Spot Detection Wizard function allowed to optimize the spot determination parameters, to quantify relative intensity of all spots and evaluate statistical significance of the measured data. Spots intensities were obtained in pixel units and normalized to the total absorbance of the gel. Significance of differences between data was tested with the non-parametric Kolmogorov–Smirnov test. Since data were normally distributed, standard deviations of these distributions were a valid parameter to assess the significance of the quantitative differences measured. The maximal value of mean and median of logarithmic ratios of standard deviations was 0.1, thus a threefold value of this parameter was used as a cut-off criterion to identify differentially expressed proteins. The increasing/decreasing index (fold change) was calculated as ratio of averaged spot intensities (relative volumes) between the investigated and control maps. Two biological replicates of each sample and three technical replicates of each biological replicate were analyzed.

In Gel Digestion and Mass Spectrometry (MS) Analysis

Spots were manually excised from gels, triturated and washed with water. Proteins were in-gel reduced, S-alkylated and digested with trypsin as previously reported [37]. Digest aliquots were removed and subjected to a desalting/concentration step on μZipTipC18 (Millipore) using 5% formic acid/50% acetonitrile as eluent before MALDI-TOF-MS or nanoLC-ESI-LIT-MS/MS analysis.

In the first case, peptide mixtures were loaded on the MALDI target, using the dried droplet technique and α-cyano-4-hydroxycinnamic acid as matrix, and analyzed by a Voyager DE PRO mass spectrometer (Applied Biosystems, Framingham, MA), operating in positive ion reflectron mode, with an acceleration voltage of 20 kV, a nitrogen laser (337 nm) and a laser repetition rate of 4 Hz. The final mass spectra, measured over a mass range of 800–4,000 Da and by averaging 50–300 laser shots, were elaborated using the DataExplorer 5.1 software (Applied Biosystems) and manually inspected to get the corresponding peak lists. Internal mass calibration was performed with peptides deriving from trypsin autoproteolysis.

In the second case, after removing acetonitrile by concentration, digests were analyzed by nanoLC-ESI-LIT-MS/MS using a LTQ XL mass

spectrometer (Thermo Finnigan, San Jose, CA) equipped with Proxeon nanospray source connected to an Easy-nanoLC (Proxeon, Odense, Denmark). Peptide mixtures were separated on an Easy C18 column (10 × 0.075 μm, 3 mm) (Proxeon, Odense, Denmark) using a linear gradient from 5% to 50% of acetonitrile in 0.1% formic acid, over 60 min, at a flow rate of 300 nl/min. Spectra were acquired in the range *m/z* 400–2000. Acquisition was controlled by a data-dependent product ion scanning procedure over the three most abundant ions, enabling dynamic exclusion (repeat count 2 and exclusion duration 1 min). The mass isolation window and collision energy were set to *m/z* 3 and 35%, respectively.

Protein Identification

MASCOT software package (Matrix Science, UK) was used to identify spots unambiguously from an updated plant non-redundant sequence database (NCBI nr 2009/05/03) in MALDI-TOF peptide mass fingerprinting experiments by using a mass tolerance value of 40–80 ppm, trypsin as proteolytic enzyme, a missed cleavages maximum value of 2 and Cys carbamidomethylation and Met oxidation as fixed and variable modification, respectively. Candidates with a MASCOT score > 82, corresponding to $P < 0.05$ for a significant identification, were further evaluated by the comparison with their calculated mass and pI values, using the experimental values obtained from 2-DE.

MASCOT software package (Matrix Science, UK) was also used to identify spots unambiguously from the same updated plant non-redundant sequence database (NCBI nr 2009/05/03) in nanoLC-ESI-LIT-MS/MS experiments by using a mass tolerance value of 2 Da for precursor ion and 0.8 Da for MS/MS fragments, trypsin as proteolytic enzyme, a missed cleavages maximum value of 2 and Cys carbamidomethylation and Met oxidation as fixed and variable modification, respectively. Candidates with more than two assigned peptides with an individual MASCOT score >25, corresponding to $P < 0.05$ for a significant identification, were further evaluated by the comparison with their calculated mass and pI values, using the experimental values obtained from 2-DE. Where appropriate, protein identification was checked manually to provide for a false positive rate <1%.

Statistical Analysis

All experiments were performed at least three times. Data from viability and lipid peroxidation assays, flow cytometry, Western blotting, RT-PCR, and transient transfection experiments were expressed as means ± SD. Statistical significance was determined by Student's test comparison between two groups of data sets. Asterisks reported in the figures show the differences of experimental groups in comparison with the corresponding control condition ($P < 0.05$, for example).

RESULTS

Cladosporol A Inhibits the Growth of Different Human CRC Cell Lines

To examine the effects of cladosporol A on cell growth, we initially treated colon carcinoma HT-29 cells for 72 h with increasing concentrations of the compound. Cell survival was reduced as evaluated by the CellTiter Aqueous One Cell Proliferation Assay (Figure 1B). The IC_{50} values of cladosporol A on HT-29 cells were 13.85, 12.35, and 6.9 μM following a 24, 48, and 72 h treatment, respectively. On the basis of these values, we tested the antiproliferative effect of cladosporol A on two additional CRC derived cell lines, CaCo-2, SW480, in parallel with HT-29. Cells were treated with increasing amounts of cladosporol A for 24 h and their proliferation rate was reduced in a dose-dependent manner (Figure 2A). HT-29 showed a more evident growth inhibition than SW480 and CaCo-2 cells and were analyzed in details in the following experiments. We then treated HT-29 cells with increasing concentrations of cladosporol A, for 4, 8, 24, and 48 h. The number of surviving cells diminished in a dose- and time-dependent manner, as compared to untreated cells (Figure 2B). Cladosporol A did not exert a generic cytotoxic effect on HT-29 cells because inhibition was reverted following drug withdrawal. Growth recovery was even more evident when cells were treated for 24 or 48 h with the drug (5 μM) and then left in culture for additional 96 h in the absence of the drug (Supplementary data1). These results are consistent with those reported by Chen et al. [33] who showed no toxicity induced by cladosporol in gastric cancer cells xenografted into nude mice. Finally, cladosporol A-treated cells detached from the plate surface with a typical rounded-up morphology as observed with a light transmission microscope (Figure 2C). All together, these findings indicate that cladosporol A inhibits the proliferative capacity of various CRC tumor cell lines, among which HT-29 cells were the most susceptible to treatment.

Cladosporol A Induces a G1-Phase Growth Arrest During the Cell Cycle

To determine the cell cycle changes underlying the growth inhibition found, the nuclear DNA content of HT-29 cells at the different phases of the cell cycle was analyzed by flow cytometry in the absence or presence of cladosporol A. HT-29 cells were cultured in proliferating medium for 24 h and, subsequently, synchronized by serum starvation for 48 h. Cells were then grown in a medium containing 10% FBS and different

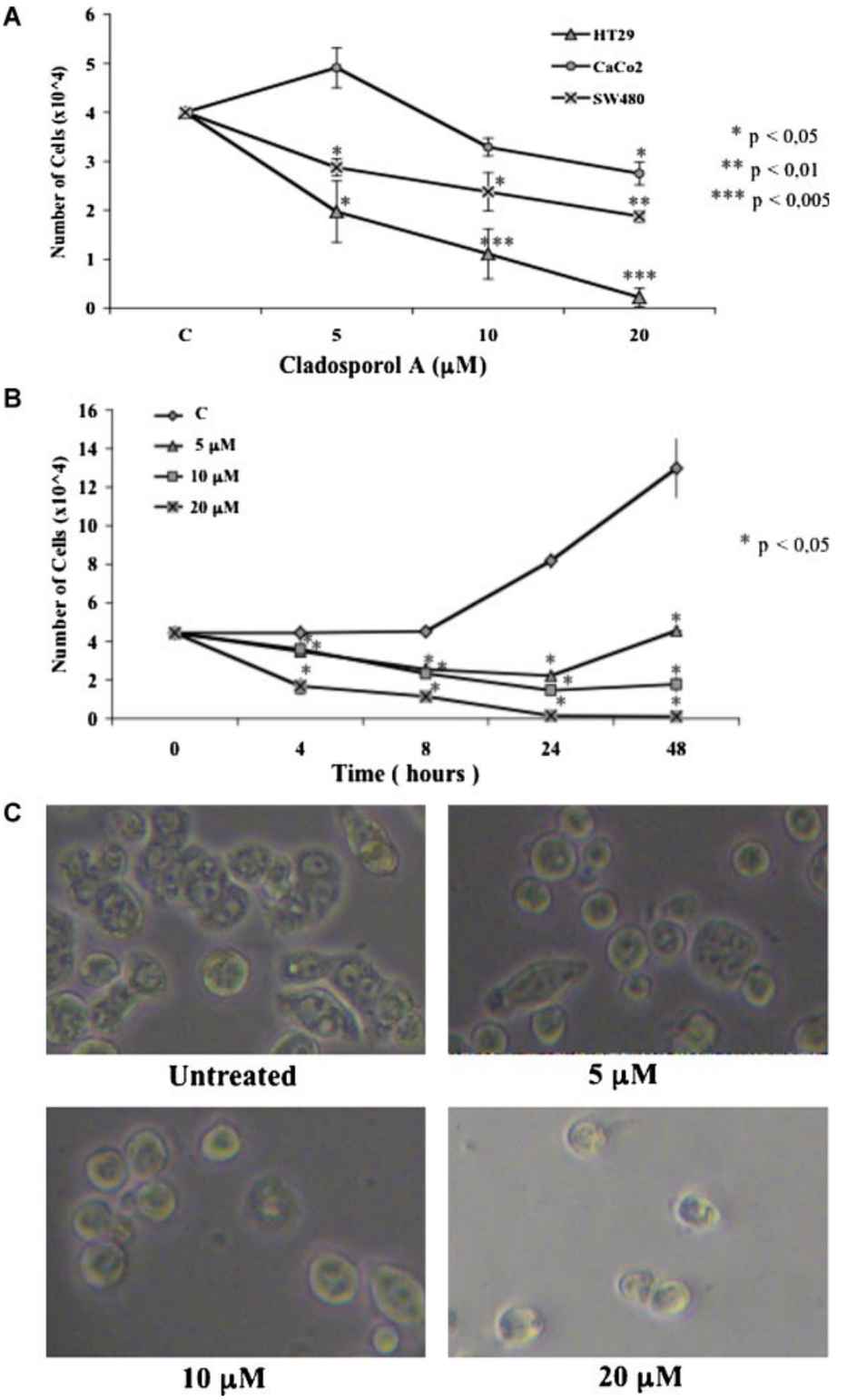

Figure 2. Cladosporol A inhibits cell growth in a dose– and time–response manner. (A) To assess the effect of cladosporol A on esponentially growing HT-29, CaCo-2, and SW480 cells, cells were treated with different doses of cladosporol A (5, 10, and 20 μM). After 24 h, cells were collected and counted. The data shown here are mean ± SD of three experiments performed in duplicate. Results were similar in two independent experiments. $^{*}P < 0.05$; $^{**}P < 0.01$; $^{***}P < 0.005$ when compared with control. (B) To assess the effect of cladosporol A on esponentially growing HT-29 cells, cells were treated or not with 5, 10, and 20 μM cladosporol A, for 4, 8, 24, and 48 h. Then, cells were collected and counted. The data shown here are mean ± SD of three experiments performed in duplicate. Results were similar in two independent experiments. $^{*}P < 0.05$ when compared with control. (C) Morphological changes of HT-29 cells treated or not with 5, 10, and 20 μM cladosporol A. Pictures were taken using light trasmission microscopy at a magnification of 10×.

concentrations of cladosporol A. Exposure to 5–10 μM of the compound determined a significant increase in the G2/M cell population and a concomitant decrease in the G1-phase cells with respect to untreated cells (Figure 3A). Specifically, treatment with 5 and 10 μM cladosporol A for 24 h resulted in 29.45% and 34.45% of G2/M cells, respectively, as compared to 19.1% of control cells (Table 1). Exposure to 20 μM cladosporol A, surprisingly, caused a significant increase of G1 cells and a parallel decrease of the S and G2/M cell population. The percentage of G1 cells was 60.2% at 12 h and 57.1% at 24 h as compared to 34.9% and 47.65% in control cells, respectively (Table 1). Cladosporol A then affects HT-29 cell proliferation ability through a cell cycle arrest at the G2/M phase at 5–10 μM or at the G1 phase at higher dosages.

We next examined whether the cell cycle arrest was associated with changes in the expression of specific proteins involved in its control (Figure 3B,C). To this aim, total protein extracts

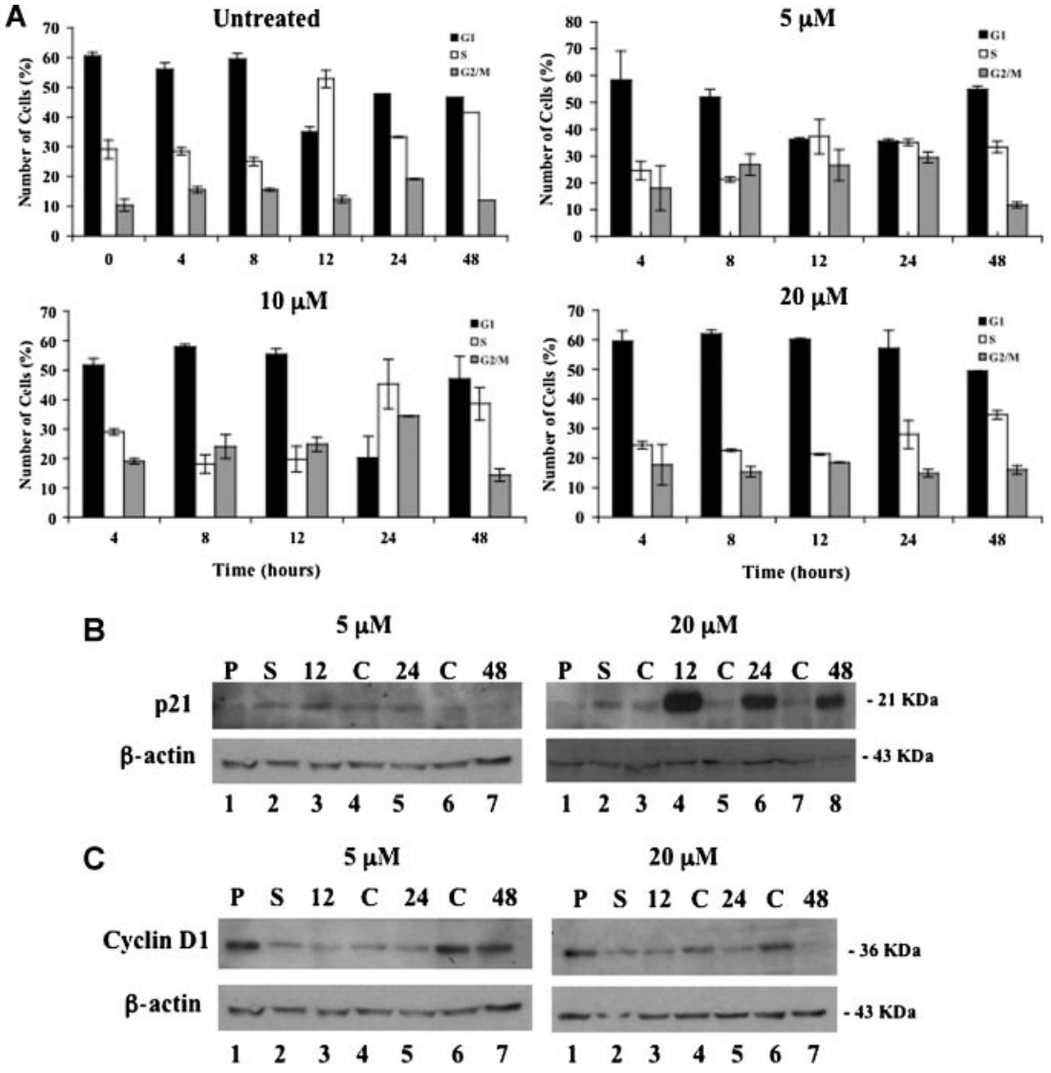

Figure 3. Cladosporol A suppresses HT-29 cells via G1-phase arrest. (A) Cell cycle distribution in HT-29 cells, firstly synchronized by serum deprivation and then treated or not with 5, 10, and 20 μM cladosporol A, for 4, 8, 12, 24, and 48 h. Data are mean ± SD of three different experiments performed in duplicate. (B) Western blotting analysis on total protein extracts produced from HT-29 cells treated or not with 5 and 20 μM cladosporol A for 12, 24, and 48 h. Anti-$p21^{waf1/cip1}$ was used to probe untreated and cladosporol A-treated HT-29 cells. Lane 1: proliferating cells; lane 2: serum-deprived cells. In lanes 4 and 6 of left panel and lanes 3, 5 and 7 of the right panel are reported the results from untreated HT-29 cells. In lanes 3, 5 and 7 of left panel and lanes 4, 6, and 8 of right panel are reported the results from HT-29 cells treated with the specific dosages for the indicated times. (C) The same samples of (B) were tested by Western blotting experiments with an anti-cyclin D1 antibody. Lane 1: proliferating cells; lane 2: serum-deprived cells. In lanes 4 and 6 of left and right panels are reported the results from untreated HT-29 cells. In lanes 3, 5, and 7 of left and right panels are reported the results from HT-29 cells treated with the specific dosages for the indicated times. To normalize the samples loaded on the gel, Western blotting with an anti-β-actin antibody was carried out.

Table 1. The Percentage of HT-29 cells in Each Population During the Cell Cycle is Reported as the Mean ± SD of Three Different Experiments Performed in Duplicate

	0 h	4 h	8 h	12 h	24 h	48 h
Untreated						
G0/G1	60.6 ± 1.1	56.5 ± 2.25	59.55 ± 1.75	34.9 ± 1.9	47.65 ± 0.15	−16.55 ± 0.65
S	29.1 ± 3.1	28.45 ± 1.25	25.04 ± 1.4	52.8 ± 3	33.2 ± 0.00	41.5 ± 0.2
G2/M	10.3 ± 2	15.5 ± 1	15.45 ± 0.45	12.3 ± 1.1	19.1 ± 0.1	12.0 ± 0.5
5 μM						
G0/G1	60.6 ± 1.1	58.25 ± 10.85	51.9 ± 3	36.15 ± 0.65	35.5 ± 0.9	54.9 ± 1.1
S	29.1 ± 3.1	24.6 ± 3.4	21.25 ± 0.95	37.2 ± 6.5	35.1 ± 1.2	33.35 ± 2.15
G2/M	10.3 ± 2	18.05 ± 8.35	26.85 ± 3.95	26.6 ± 5.8	29.45 ± 2.05	11.75 ± 1.05
10 μM						
G0/G1	60.6 ± 1.1	51.75 ± 2.25	57.85 ± 0.95	55.4 ± 1.9	20.3 ± 7.2	47 ± 7.7
S	29.1 ± 3.1	29 ± 1	18.1 ± 3.1	19.8 ± 4.4	45.3 ± 8.4	38.6 ± 5.5
G2/M	10.3 ± 2	19.05 ± 0.95	24.05 ± 4.05	24.8 ± 2.5	34.45 ± 0.15	14.4 ± 2.2
20 μM						
G0/G1	60.6 ± 1.1	59.65 ± 3.55	62 ± 1.4	36.15 ± 0.65	35.5 ± 0.9	54.9 ± 1.1
S	29.1 ± 3.1	24.35 ± 1.25	22.65 ± 0.35	52.8 ± 3	33.2 ± 0.00	41.5 ± 0.2
G2/M	10.3 ± 2	17.7 ± 6.8	15.35 ± 1.75	18.5 ± 0.00	14.9 ± 1.3	16 ± 1.5

For all treated samples *P*-values were calculated ($P < 0.05$ when compared with control).

from HT-29 proliferating (lane 1), serum-deprived (lane 2), treated with 5 μM (lanes 3, 5, and 7, left panel) and 20 μM cladosporol A (lanes 4, 6, and 8, right panel), for 12, 24, and 48 h, were probed for $p21^{waf1/cip1}$ by Western blotting and compared to untreated control cells (lanes 4 and 6 for the 5 μM dosage, left panel; lanes 3, 5, and 7 for the 20 μM dosage, right panel). $p21^{waf1/cip1}$ was expressed at high levels in HT-29 cells treated with 20 μM cladosporol A for 12 h (Figure 3B, right panel lane 4), and only modestly in proliferating cells (lane 1) and corresponding controls at 12, 24, and 48 h (lanes 3, 5 and 7). The expression remained elevated in cells exposed to 20 μM cladosporol A for 24 and 48 h (lanes 6 and 8), although progressively diminished, suggesting degradation events. In serum-deprived cells, $p21^{waf1/cip1}$ expression was only slightly increased, as expected (lane 2). Cyclin D1 expression was lower in cells treated for 24 and 48 h with 20 μM cladosporol A (lanes 5 and 7) than the untreated controls (lanes 4 and 6), confirming the specific G1-phase block (Figure 3C, right panel). No changes in $p21^{waf1/cip1}$ or cyclin D1 protein expression were observed in HT-29 cells exposed to 5 μM cladosporol A, in agreement with the flow cytometry data (see Figure 3A–C). Thus, the treatment with 20 μM cladosporol A causes a G1 phase arrest as documented by the increase in $p21^{waf1/cip1}$ expression and the simultaneous decrease of cyclin D1.

Cladosporol A Influences the Expression of Cell Cycle Regulators in Proliferating HT-29 Cells

We then treated proliferating HT-29 cells for different times with increasing concentrations of cladosporol A and assessed the expression of specific proteins involved in cell-cycle control. Expression of $p21^{waf1/cip1}$, cyclin A and B1, specific markers of G1, S, and G2/M phases, respectively, was investigated by Western blotting assay. Exposure to 5–10 μM cladosporol A for 4 and 8 h, resulted in a modest increase of $p21^{waf1/cip1}$, whereas the treatment with 20 μM cladosporol A, for the same times, caused a robust accumulation of $p21^{waf1/cip1}$ (Figure 4). From 8 h of treatment, $p21^{waf1/cip1}$ started to decline to reach undetectable levels at 48 h. Cyclin B1 expression increased in a dose (5, 10, and 20 μM) and time dependent manner (4, 8, and 24 h), recovering the control levels at 48 h. Cyclin A expression, on the contrary, rapidly diminished already at 4 h of treatment with 5, 10, and 20 μM cladosporol A, with no detectable variations at 8, 24, and 48 h.

Since $p21^{waf1/cip1}$ accumulates in proliferating HT-29 cells after only 4 h of cladosporol A exposure, we next investigated whether other cell cycle regulators were affected under the same experimental conditions. Cells were treated with 20 μM cladosporol A, for 4, 6, and 8 h, and protein extracts analyzed by Western blotting for different cell cycle gatekeepers (Figure 5A–I). In addition to the growth arrest, accumulation of $p21^{waf1/cip1}$ protein (about twofold as compared to control) and progressive decrease of cyclin D1 as shown above, cyclin B1 showed a light increase while Cdc2-p34 and PCNA slightly decreased suggesting a partial accumulation of cells at the G2/M phase. This block occurred even if the treatment with 20 μM cladosporol A was associated with a G1 phase arrest. Moreover, cyclin E, CDK2, CDK4 also showed

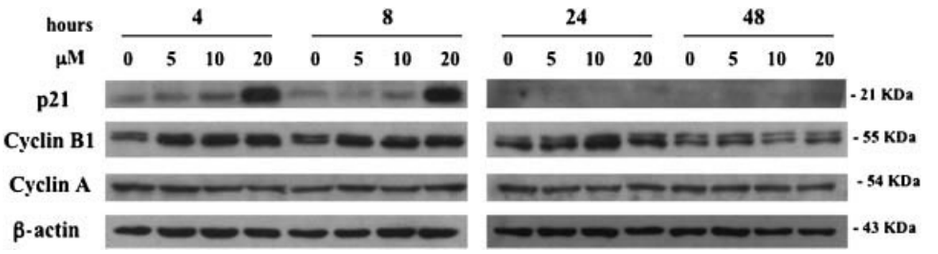

Figure 4. Effect of cladosporol A on the cell cycle regulators expression in proliferating HT-29 cells treated or not with 5, 10, and 20 μM cladosporol A, for 4, 8, 24, and 48 h. Different antibodies against $p21^{waf1/cip1}$, cyclin B1 and cyclin A, three modulators of G1, S, and G2/M phases, respectively, were used in the Western blotting analysis. To control the samples loaded derived from untreated and cladosporol A-treated HT-29 cells, an anti-β-actin antibody was used. Cells were treated with the specific dosages for the indicated times.

a time-dependent decrease indicating that inhibition of cyclinD1/CDK4 and cyclinE/CDK2 complexes might explain the cladosporol A-induced G1 phase cell cycle arrest (Figure 5F–H). As shown in Figure 5L, treatment of HT-29 cells with 20 μM of cladosporol A resulted in a reduction in histone H1-associated CDK2 activity that could be due to the cyclin E and CDK2 decrease, and simultaneous increase of cyclinE/CDK2 complex binding to CDKIs, that is, $p21^{waf1/cip1}$. Lastly, RB, which is the target of the cyclinD1/CDK4, showed a significant reduction after cladosporol A treatment, suggesting a diminished availability to the binding with cyclinD1/CDK4 complex (Figure 5I). Together, these results indicate that cladosporol A is responsible for the changes in cell cycle regulators not only in synchronized, but also in proliferating HT-29 cells and, remarkably, that the cladosporol A-induced G1 phase cell cycle arrest in HT-29 cells could be sequentially caused by induction of CDKIs ($p21^{waf1/cip1}$), a decrease of G1 phase cyclins and CDKs and, finally, a decrease in the histone H1-associated CDK2 kinase activity.

Cladosporol A Up-regulates $p21^{waf1/cip1}$ Transcription in HT-29 Cells

To investigate whether the $p21^{waf1/cip1}$ increase was due to a gene transcription activation, total RNA was extracted from HT-29 cells treated with 20 μM cladosporol A, for 1, 2, 4, and 8 h, and analyzed by semiquantitative RT-PCR. The $p21^{waf1/cip1}$ specific amplicon showed a sharp increase after 2 h reaching a plateau at 4 and 8 h (Figure 6A). Similar results were obtained by carrying out longer PCR assays (30 vs. 35 cycles) (Figure 6B). A more accurate analysis by RT-qPCR further supported these results as illustrated in Figure 6C.

To confirm that cladosporol A induces a more efficient $p21^{waf1/cip1}$ gene transcription, we transiently transfected proliferating HT-29 cells with a recombinant plasmid (pWWP) bearing the entire $p21^{waf1/cip1}$ human gene promoter, a 2,320 bp long fragment, fused upstream to the luciferase reporter gene [38]. Exposure of transfected HT-29 cells to 20 μM of cladosporol A caused an increase in luciferase activity as compared to untreated cells (Figure 6D). Note that no luciferase activity was detected at higher cladosporol A concentrations indicating that transcription inhibition is likely due to a drug saturation effect. As a positive control, an aliquot of transfected cells was exposed to 10 μM troglitazone, a member of the thiazolidinediones (TZD) family of PPARγ specific ligands. In fact, it is known that the human $p21^{waf1/cip1}$ gene is positively regulated through the interaction of the transcription factor Sp1 with PPARγ▽ a member of the orphan nuclear receptors family [38–40], particularly in thyroid cells [41].

To investigate whether the Sp1 binding sites located in proximal promoter play any role in mediating cladosporol A-induced $p21^{waf1/cip1}$ gene transcription, we transiently transfected a reporter construct (pWP124) that includes only the more proximal 124 bp of the $p21^{waf1/cip1}$ promoter and no longer carries the two p53 binding sites located at position −2301 and −1394 and the two RXR motifs at −1221 (RXRE1) and −1198 (RXRE2), respectively (Figure 6E). Luciferase activity in cells treated with cladosporol A was higher than that observed in cells transfected with the reporter plasmid carrying the entire promoter (pWWP), suggesting that the transcriptional efficiency of the human $p21^{waf1/cip1}$ promoter depends on the presence of the Sp1 binding motifs located within the proximal promoter. Neither the binding of p53 nor that of RXR to their cognate motifs in the more upstream promoter appear to be required for cladosporol A-induced $p21^{waf1/cip1}$ transcription.

To understand the relative contribution of the Sp1 binding sites to gene activation, we transiently transfected recombinant plasmids in which the Sp1 binding sites were either deleted or site-directed mutated (Figure 6E). Plasmid pWP101, carrying a shorter version of the $p21^{waf1/cip1}$ promoter in which the two more upstream Sp1

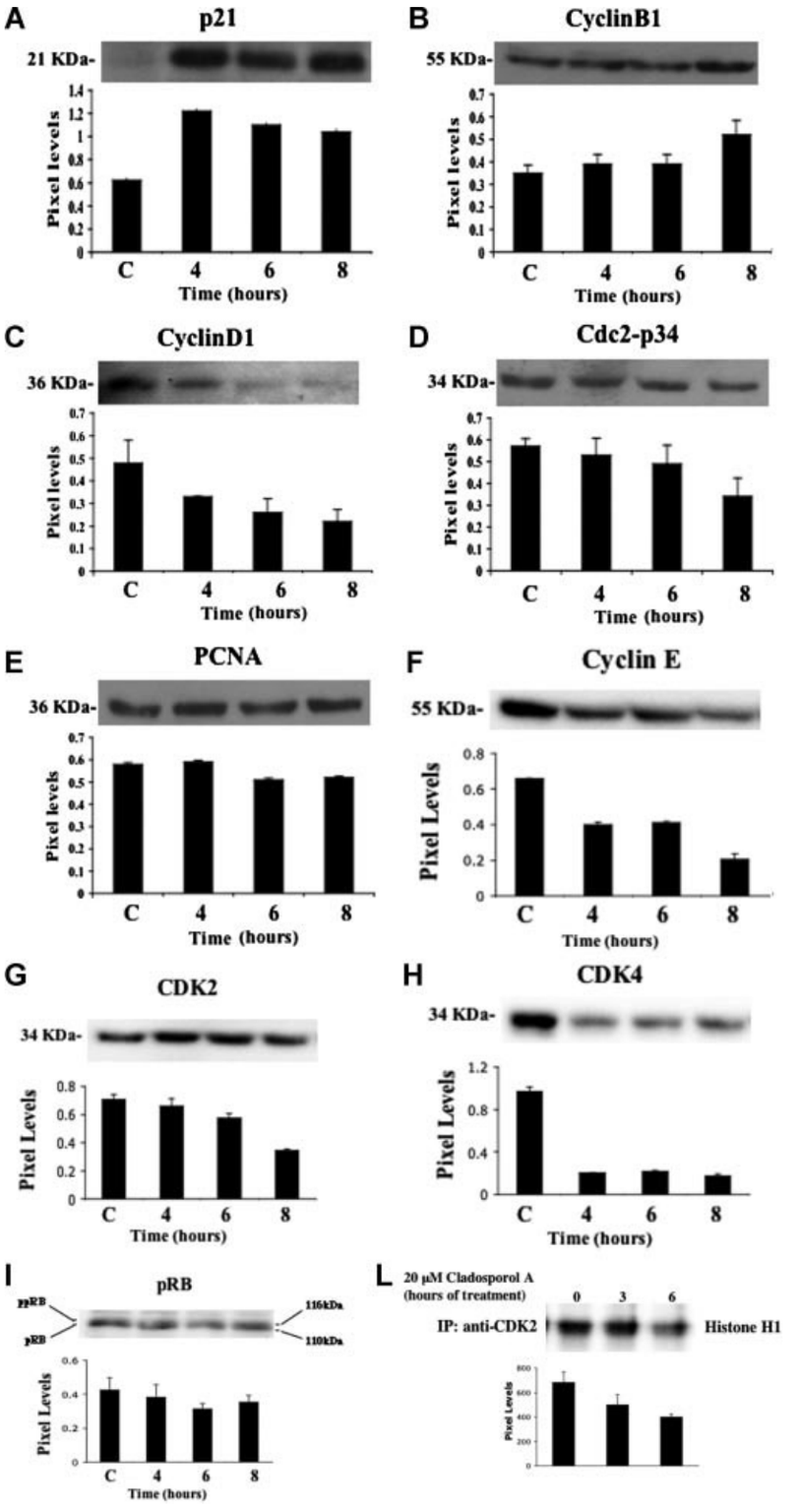

Figure 5. Quantitative evaluation of the cladosporol A-induced expression of the cell cycle regulators in proliferating HT-29 cells. Cells were treated or not with 20 μM cladosporol A, for 4, 6, and 8 h. Cell lysates were prepared in non-denaturing lysis buffer and then analyzed by Western blotting using anti-$p21^{waf1/cip1}$ (A), anti-cyclin B1 (B), anti-cyclin D1 (C), anti-Cdc2-p34 (D), anti-PCNA (E), anti-cyclin E (F), anti-CDK2 (G), anti-CDK4 (H), anti-RB (I) antibodies. To control the samples loaded derived from untreated and cladosporol A-treated HT-29 cells, an anti-β-actin antibody was used. The bar graphs represent the mean ± SD of proteins/β-actin of at least three independent experiments. The Western blotting assays reported here are representative of a single exemplificative experiment. (L) Histone H1-associated CDK2 kinase activity assay in proliferating HT-29 cells. Cells were treated with 20 μM cladosporol A for the indicated times and then total cell lysates of each sample were immunoprecipitated with anti-CDK2 antibody. The kinase reaction was performed using histone H1 as substrate of cyclin E/CDK2 complex. The bar graphs represent the mean ± SD of at least three independent experiments, while the assay reported here is representative of a single exemplificative experiment.

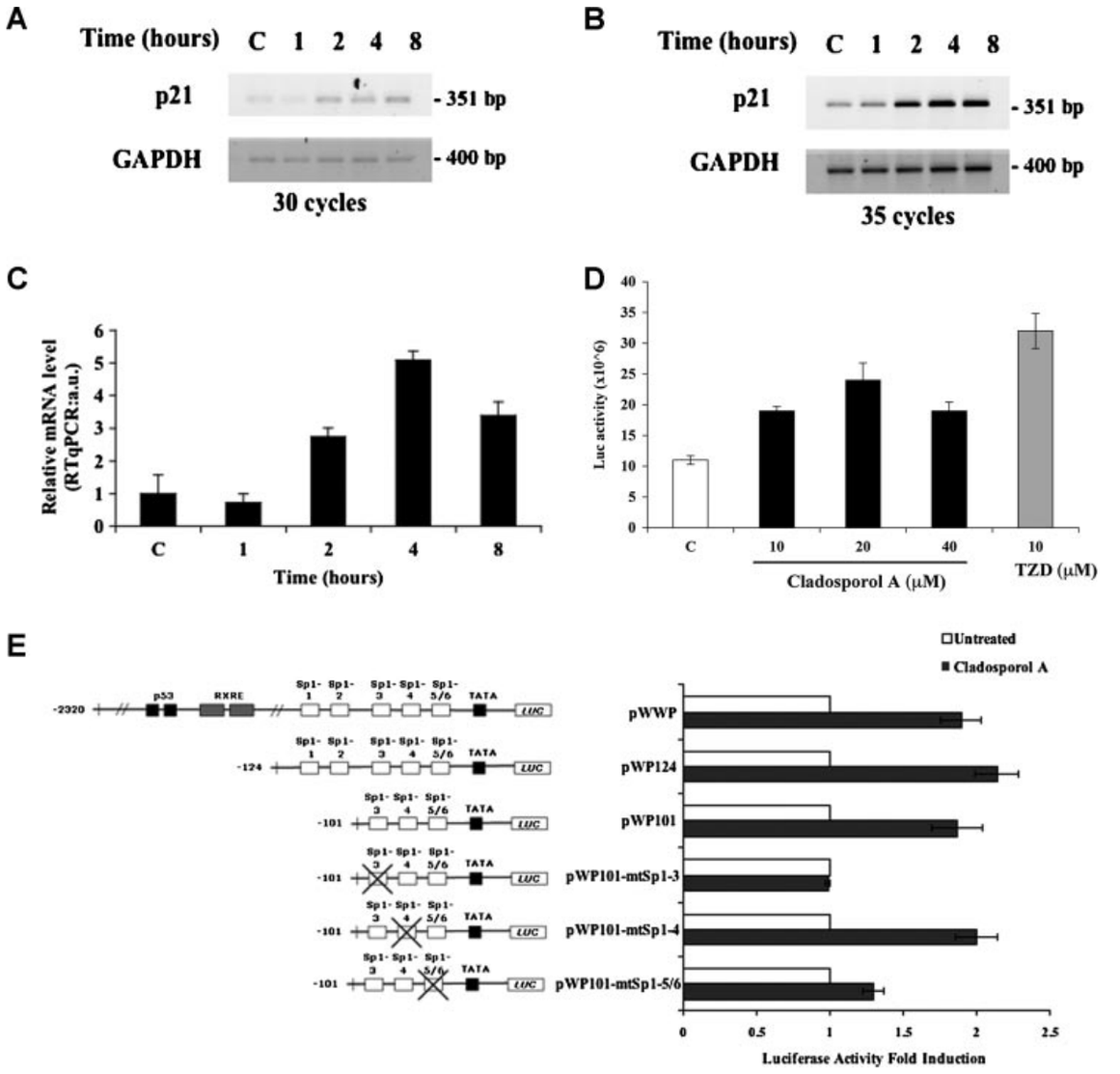

Figure 6. Cladosporol A treatment induces the p21$^{waf1/cip1}$ gene transcription. (A) mRNA expression of p21$^{waf1/cip1}$ in HT-29 cells evaluated by semiquantitative RT-PCR. Total RNA extracted from proliferating HT-29 cells treated or not with 20 μM of cladosporol A, for 1, 2, 4, and 8 h, was used to amplify the specific p21$^{waf1/cip1}$ 351 bp-long product for 30 cycles. Amplification of the GAPDH gene was used as internal control. (B) The same total RNA samples of (A) were used to amplify the specific p21$^{waf1/cip1}$ 351 bp-long amplification product for 35 cycles. Amplification of the GAPDH gene was used as internal control. (C) Real-time RT-qPCR was performed using total RNA extracted from proliferating HT-29 cells treated or not with 20 μM of Cladosporol A for 1, 2, 4, and 8 h. The bar graphs represent the mean ± SD of p21$^{waf1/cip1}$/GAPDH produced after three independent experiments. (D) Cladosporol A induces transcriptional activity of p21$^{waf1/cip1}$ promoter gene. HT-29 cells were transiently transfected with the wild-type p21$^{waf1/cip1}$ promoter-luciferase plasmid (pWWP) reported in panel E and treated with 10, 20, and 40 μM of cladosporol A for 24 h. TZD (10 μM) was used as positive control of p21$^{waf1/cip1}$ promoter transcriptional activity. Luciferase activities were normalized to the β-galatosidase ones used as control. Data shown are mean ± SD of three independent experiments performed in duplicate. (E) Functional analysis of the transcriptional activity of p21$^{waf1/cip1}$ promoter gene by deletion and site-directed mutagenesis. Left: structural features of the recombinant plasmids carrying the mutated forms of the p21$^{waf1/cip1}$ promoter used in this study. Right: results of the transiently transfections in HT-29 cells as fold induction of luciferase activity and obtained with the p21$^{waf1/cip1}$ promoter-luciferase plasmids reported in the left panel. Cells were treated with 20 μM of cladosporol A for 24 h. The luciferase activities were normalized to the β-galatosidase ones used as control. Data shown are mean ± SD of three independent experiments performed in duplicate.

binding sites (Sp1-1 and Sp1-2) were deleted, was still able to respond to 20 μM cladosporol A-treatment with an increase of luciferase activity similar to that observed with plasmids pWP124 and pWWP. Transfection of the pWP101-mtSp1-3, in which the third Sp1 binding site is mutated, caused only a slight induction of luciferase activity. Plasmid pWP101-mtSp1-4 with a mutated binding site 4 did not affect the luciferase activity increase of the intact 124 bp long promoter,

whereas plasmid pWP101-mtSp1-5/6 with mutated Sp1 binding sites 5/6 caused a very low, if any, luciferase activity. These results indicate that the two more upstream Sp1 binding sites do not affect $p21^{waf1/cip1}$ transcriptional efficiency, while the Sp1 binding sites 3 and 5/6 appear to play a central role in mediating the formation of a transcriptional apparatus capable to promote gene expression.

Cladosporol A Treatment of HT-29 Cells Induces an Oxidative Stress-Response and Activates the MAPK Pathways

To further investigate the protein variations induced by cladosporol A in HT-29 cells, a proteomic analysis was performed on cells treated or not with 20 μM cladosporol A for 8 h. Total protein extracts were separated on PAGEs covering a 4–7 pH range and 10–150 kDa Mr ranges, followed by a Coomassie-based reagent staining. All gel images from treated and untreated cells were acquired and quantitatively evaluated (Supplementary data 2). About 30 spots showed at least a twofold difference in relative absorbance between samples; 21 spots were associated to protein sequence entries by different MS approaches (Supplementary data 3). Chaperones, structural proteins, transcription and translation factors, cell cycle regulators, redox response modulators and apoptotic proteins were identified among those whose expression changes after cladosporol A treatment.

To confirm that the protein changes observed after drug treatment were dependent upon an oxidative stress response, total protein extracts from proliferating HT-29 cells exposed to 20 μM cladosporol A, for 4, 6, and 8 h were analyzed by Western blotting with antibodies recognizing the phosphorylated forms of ERK and JNK. Both proteins increased after treatment (Figure 7A,B). To demonstrate that both signaling pathways mediate the cladosporol A-induced redox response, we then treated HT-29 cells as above in the presence or absence of increasing concentrations of NAC (*N*-acetyl-cysteine), an inhibitor of redox species accumulation. Exposure to 20 μM cladosporol A caused a simultaneous increase in $p21^{waf1/cip1}$, pERK, and pJNK, while addition of increasing concentrations of NAC counteracted the drug-induced increase of the three proteins (Figure 7C).

To further prove the redox species enhancement by cladosporol A treatment, we assessed MDA production through a lipid peroxydation assay as well as the involvement of the NADPH oxydase, the main enzymatic machinery responsible of ROS generation. An increase in the production of reactive species was firstly observed, confirming that cladosporol A induces a redox response (Supplementary data 4A). Afterwards, we analyzed whether the cladosporol A-induced ROS generation was prevented by the NADPH oxidase specific inhibitor apocynin. The results shown in Supplementary data 4B demonstrate that preincubation with apocynin, before cladosporol A exposure, results in a reduced $p21^{waf1/cip1}$ expression, suggesting that cladosporol A induces NADPH oxidase-dependent ROS generation.

Finally, to further demonstrate the functional link between ERK pathway and $p21^{waf1/cip1}$ expression, we treated HT-29 cells with two MEK inhibitors, PD98059 and UO126. The results indicated that $p21^{waf1/cip1}$ was up-regulated only when the pathway is functional; when pERK was blocked, no $p21^{waf1/cip1}$ increase was observed (Figure 7D).

These results provide the first evidence that ERK (and JNK also) might function as mediator of the cladosporol A-induced inhibition of HT-29 cell growth. Although additional experiments must be performed to clarify the interplay between the different signaling pathways activated by cladosporol A, our preliminary data suggest that the mitogen-activated protein kinase (MAPK) pathways are involved in the cladosporol A-induced regulation of HT-29 cells proliferation.

DISCUSSION

In this paper, we provide evidence that cladosporol A displays antiproliferative activity in human CRC derived cell lines, specifically in HT-29 cells (Figures 1B and 2A–C). The inhibition of cell proliferation is reversible at lower doses (5 and 10 μM), as the cells can escape the cell cycle arrest; in contrast, cell proliferation is irreversibly reduced at higher doses (20 μM) (Figure 2B), suggesting that cladosporol A could act as a cytostatic rather than a cytotoxic compound in human CRC derived cells (Figure 2B and Supplementary data 1). Similar results were obtained in other cell lines of the same origin; the effects were more pronounced in HT-29, likely due to their different genotypes that could impart a different response to the drug (for details see in Materials and Methods Section).

Inhibition of cell growth by cytostatic agents is generally accompanied by a cell cycle arrest at specific phases. Higher doses of cladosporol A were associated with a specific G1 phase arrest, while, surprisingly, lower doses were associated with cell accumulation at the G2/M phase (Figure 3 and Table 1). Other molecules can cause both a G1 and a G2/M arrest at different concentrations. Quercetin, a flavonoid derived from grape, caper, red onion, and green tea, induces a G2/M arrest at lower (14.8 μM) and a G1 arrest at higher concentrations (52.1 μM) [42]. Silibinin, the major component of milk thistle extract isolated from

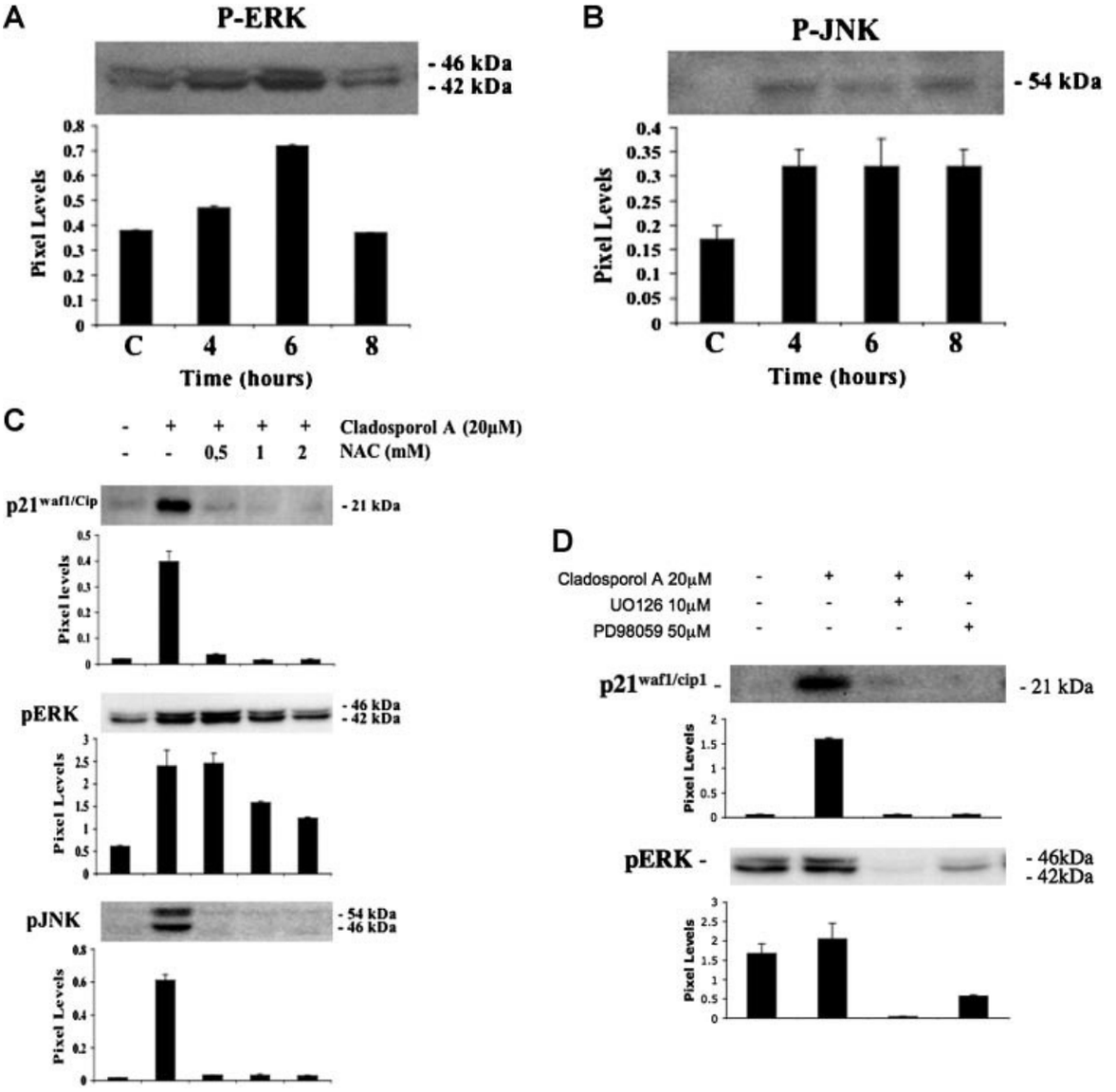

Figure 7. Cladosporol A treatment of HT-29 cells induces an oxidative stress–response and activates the MAPK pathways. Cells were treated or not with 20 μM cladosporol A, for 4, 6, and 8 h. Cell lysates were prepared in non-denaturing lysis buffer and then analyzed by Western blotting using antibodies specifically recognizing the phosphorylated forms of ERK (A) and JNK (B) or β-actin (control). The bar graphs represent the mean ± SD of pERK or pJNK/β-actin of three independent experiments. Western blotting assays reported here are representative of a single exemplificative experiment. (C) Cells were treated or not with 20 μM cladosporol A, for 4 h in absence and presence of increasing concentrations of NAC (*N*-acetyl-cysteine). Cell lysates were prepared in non-denaturing lysis buffer and then analyzed by Western blotting using antibodies specifically recognizing the phosphorylated forms of $p21^{waf1/cip1}$, pERK, and pJNK. The bar graphs represent the mean ± SD of $p21^{waf1/cip1}$ or pERK or pJNK/β-actin of three independent experiments. Western blotting assays reported here are representative of a single exemplificative experiment. (D) Cells were treated or not with 20 μM cladosporol A, for 4 h in absence and presence of UO126 10 μM and PD98059 50 μM. Cell lysates were prepared in non-denaturing lysis buffer and then analyzed by Western blotting using antibodies specifically recognizing $p21^{waf1/cip1}$ and pERK. The bar graphs represent the mean ± SD of p21 or pERK /β-actin of three independent experiments. Western blotting assays reported here are representative of a single exemplificative experiment.

Sylibum marianum, on the contrary, induces a G1 arrest at lower concentrations (50 and 75 μM), whereas provokes a G2/M block at higher concentrations (100 μM) [43].

The G2/M phase arrest that mainly occurs in cells bearing DNA damages, allows these injuries to be repaired before cells proceed into mitosis, thereby preventing the stabilization of the mutations. Accumulation of cells at the G2/M phase observed with lower dosage suggests that cladosporol A somehow inhibits DNA replication.

On the contrary, at higher dosage, cladosporol A hits different molecular targets as documented by changes in the expression of $p21^{waf1/cip1}$ and cyclin D1 (Figure 3). $p21^{waf1/cip1}$ is considered as the universal inhibitor of cell cycle progression: it is up-regulated in G1 and in G2/M phase and this bimodal periodicity of expression suggests a role in the control of both phases of the cell cycle [44]. The robust increase in $p21^{waf1/cip1}$ expression, which we found in cells blocked at G1 phase, likely indicates that, in our case, $p21^{waf1/cip1}$ exerts its effect in this phase (Figure 3B).

In proliferating HT-29 cells, indeed, we also found a remarkable reduction in cyclin D1, cyclin E, CDK2, and CDK4 expression after cladosporol A treatment (Figures 4 and 5), proteins largely involved in the G1/S restriction point control. All together, a down-expression of cyclin D1, cyclin E, CDK2, and CDK4 and a simultaneous over-expression of $p21^{waf1/cip1}$ appears to influence the $p21^{waf1/cip1}$ ability to bind the cyclinE/CDK2 complex and, consequently, to generate a reduced kinase activity. The data reported in Figure 5L demonstrate that the cyclinE/CDK2 complex, that peaks at G1/S transition and usually phosphorylates several proteins, after cladosporol A treatment, is not longer able to phosphorylate the histone H1, confirming the inhibition of the G1/S transition and the cell cycle arrest in HT-29 cells.

In proliferating HT-29 cells, the increased $p21^{waf1/cip1}$ expression is accompanied by reduced levels of cyclin D1 and PCNA (Figures 3–5), confirming the role they play in regulating the G1/S progression. Indeed, $p21^{waf1/cip1}$ binds the cyclin D1-CDK4/CDK6 complexes and inhibits their kinase activity toward RB protein, stimulating a proteasomal degradation of the complexes and promoting a proliferation arrest [45]. Since we found a reduced expression of RB protein expression after cladosporol A treatment (Figure 5I), it is conceivable that this event results in an attenuated RB-associated cyclin D1/CDK4 kinase activity. $p21^{waf1/cip1}$ is also a strong inhibitor of the DNA polymerase auxiliary protein, PCNA, through its carboxy-terminal domain [46]. The diminished expression of PCNA, shown in Figure 5E, is the demonstration of the cladosporol A-induced action of $p21^{waf1/cip1}$.

Cyclin B1 and Cdc2-p34, known markers of the G2/M arrest, are also reduced, suggesting that cladosporol A at higher doses probably overcomes the effects induced by lower doses (Figure 5B,D). However, we cannot exclude that, even at higher doses, HT-29 cells are partially arrested at the G2/M phase as documented by the reduction of the Cdc2-p34 protein (Figure 5D). More experiments are required to study the detailed mechanisms by which cladosporol A inhibits HT-29 cell proliferation through the G2/M phase arrest.

$p21^{waf1/cip1}$ expression is finely regulated by different mechanisms at the post-transcriptional level; however, the most efficient way to modulate its expression occurs at the transcriptional level through both p53-dependent and p53-independent mechanisms that involve a variety of factors [38]. p53, in turn, trans-activates several genes involved in growth control and the presence of two p53-responsive elements in the promoter region of the mouse, rat and human $p21^{waf1/cip1}$ genes suggests a role for this protein in transcription activation after DNA damage [38]. Other stimuli (RAS, c-Rel, Neu Diff. Factor, Zta, ribonucleotide inhibitors) can induce $p21^{waf1/cip1}$ gene expression through up-regulation and/or stabilization of the p53 protein [38]. Also, induction of p53-independent $p21^{waf1/cip1}$ gene transcription requires the activation of transcription factors by different stimuli and binding to their cognate sequences in the promoter region. Phorbol ester (PMA) and okadaic acid induce $p21^{waf1/cip1}$ gene transcription by stimulating Sp1 binding to the corresponding response elements in human leukemic cell U937 [47]. Also butyrate, transforming growth factor-β (TGF-β), lovastatin, trichostatin A, and NGF induce $p21^{waf1/cip1}$ gene transcription. Indeed, several Sp1 binding sites are clustered within the 120 bp proximal to the transcription start site in the $p21^{waf1/cip1}$ human gene promoter; in all cases, the role of the Sp1 site 3 resulted to be crucial [36,48–51]. The experiments presented here (Figure 6) clearly show that a major role in $p21^{waf1/cip1}$ induction by cladosporol A is played by Sp1 and not by p53. Deletion of the p53 binding sites did not affect the response, whereas deletion or site-directed mutants of the Sp1binding sites caused a dramatic reduction of $p21^{waf1/cip1}$ reporter gene expression (Figure 6E). Note that HT-29 cells bear a mutated form of p53 and, in fact, we observed no significant variations in p53 expression after cladosporol A treatment (20 μM for 4, 6, and 8 h) (Supplementary data 5). In addition, we tested the effects of cladosporol A both in p53 +/+ and p53−/− HCT116 cells. Despite a difference in basal $p21^{waf1/cip1}$ protein levels, the relative increase in $p21^{waf1/cip1}$ expression, which we detected in both cells, was similar, confirming that the presence of a functional p53 is not required (Supplementary data 6). The increase in $p21^{waf1/cip1}$ expression is associated to the G1 phase arrest also in cladosporol A-treated p53 +/+ and p53−/− HCT116 cells as reported in Supplementary Data 7. Both cell types are blocked in G1 phase, even if only for 12 h, and then they start again to progress in the cell cycle, demonstrating that the G1 arrest does not depend on p53. The shorter cell cycle arrest observed in both p53 +/+ and p53−/− HCT116 cells could be

due to the different cellular context in which cladosporol A exerts its action.

Although we definitively demonstrated that activation of $p21^{waf1/cip1}$ gene transcription by cladosporol A in HT-29 cells involves a p53-independent pathway, we cannot exclude that other mechanisms and protein factors may be involved in the G1 phase arrest and inhibition of cell proliferation observed, in addition to the gene expression variations reported. To this aim, we analyzed changes in the HT-29 cells proteome, following treatment with cladosporol A and found that the steady state of several proteins was modified (Supplementary Data 3). Interestingly, among these, some play a central role in controlling the oxidative stress response of the cell. Specifically, the MAPK cascades, such as ERK, JNK, and p38 pathways, are activated in response to oxidant species accumulation after administration of chemiopreventive agents. We provide evidence that higher doses of cladosporol A stimulate an oxidative stress via different mechanisms and induce an adaptative response through activation of the ERK and JNK pathways (Figure 7), resulting in a $p21^{waf1/cip1}$ increase, cyclin D1 decrease, G1 phase arrest and reduced cell proliferation. Recent reports demonstrated that cyclin D1 expression and p53-independent $p21^{waf1/cip1}$ induction are modulated through the MAPK pathways in various cell lines [52,53]. Although the data obtained by proteome analysis need to be expanded, they indicate that other factors could, directly or indirectly, be targeted by the treatment and that intricate mechanisms could integrate the different actions of cladosporol A in controlling cancer cell proliferation.

In summary, in this work we demonstrated that cladosporol A is responsible for a diminished CRC cells proliferation, especially in HT-29 cells, caused by a G1 phase arrest and determined by the simultaneous increase of $p21^{waf1/cip1}$ and decrease of several cell cycle regulators. The enhanced $p21^{waf1/cip1}$ protein levels are generated by an intense Sp1-dependent, p53-independent $p21^{waf1/cip1}$ induction of gene transcription. The results of this work demonstrate for the first time that ERK (and JNK also) might function as mediator of the cladosporol A-induced inhibition of HT-29 cell growth, suggesting the existence of a regulatory circuit that integrates cell cycle regulation and the signaling pathways both converging towards inhibition of cell proliferation.

ACKNOWLEDGMENTS

Authors thank Dr. Y. Sowa for the gift of the recombinant plasmids of $p21^{waf1/cip1}$ promoter region. This work was partially supported by grants from MIUR (PRIN2006 to V. C.). This work was partially supported by grants from MIUR (FIRB-RBNE08YFN3, PRIN 2008CCPKRP_002/003) and Regione Campania (Rete di Spettrometria di Massa–RESMAC) to A.S.

REFERENCES

1. Milner JA. Molecular target for bioactive food components. J Nutr 2004;134:2492S–2498S.
2. Chen C, King A. Dietary cancer-chemopreventive compounds: From signalling and gene expression to pharmacologica. Trends Mol Med 2005;26:318–328.
3. Manson M, Farmer P, Gensher A, Steward W. Innovative agents in cancer prevention Recent Results Cancer Res 2005;166:257–275.
4. Nasini G, Arnone A, Assante G, Bava A, Moricca S, Ragazzi A. Secondary metabolites of Cladosporium tenuissimum, a hyperparasite of rust fungi. Phytochemistry 2004;65:2104–2111.
5. Moricca S, Ragazzi A, Mitchelson KR. Molecular and conventional detection and identification of *Cladosporium tenuissimum* on two-needle pine rust aeciospores. Can J Bot 1999;77:339–347.
6. Sakagami Y, Sano A, Hara O, Mikawa T, Marumo S. Cladosporol, β–1,3–glucan biosynthesis inhibitor, isolated by the fungus *Cladosporium cladosporioides*. Tetrahedron Lett 1995;36:1469–1472.
7. Fukushima Y, Sakagami Y, Marumo S. β-glucan biosynthesis inhibitors isolated from fungi as hyphal malformation inducers. Bioorganic Med Chem Lett 1993;3:1219–1222.
8. Sakagami Y, Sano A, Marumo S, Yoshikawa N, Nakagawa J. Cladosporol, a plant growth regulator produced by fungus *Cladosporium cladosporioides*. Tennen Yuki Kagobutsu Toronkai Koen Yoshishu 1992;34:134–141.
9. Moricca S, Ragazzi A, Mitchelson KR, Assante G. Antagonism of the two-needle pine stem rust fungi *Cronartium flaccidum* and *Peridermium pini* by *Cladosporium tenuissimum* in vitro and in planta. Phytopathology 2001;91:457–468.
10. Moricca S, Ragazzi A, Assante G. Biocontrol of rust fungi by *Cladosporium tenuissimum*. In: Hao Pei M, McCracken AR, editors. Rust diseases of willow and poplar. International, Wallingford, UK: CABI Publishing; 2005. pp. 213–229.
11. Assante G, Bava A, Nasini G. Enhancement of a pentacyclic tyrosine kinase inhibitor production in *Cladosporium* cf. *cladosporioides* by Cladosporol. Applied Microbiol Biotechnol 2006;69:718–721.
12. Jemal A, Siegel R, Ward E, Hao Y, Thun MJ. Cancer statistics. CA Cancer J Clin 2009;4:225–249.
13. Samowits WS, Curtin K, Ma KN, et al. Prognostic significance of p53 mutations in colon cancer at the population level. Int. J Cancer 2002;99:597–602.
14. Sebolt-Leopold JS, Dudley DT, Herrera R, et al. Blockade of the MAP kinase pathway suppresses growth of colon tumors in vivo. Nat Med 1999;5:810–816.
15. Torrance CJ, Jackson PE, Montgomery E, et al. Combinatorial chemoprevention of intestinal neoplasia. Nat Med 2000;6:1024–1028.
16. Buolamwini JK. Cell cycle molecular target in novel anticancer drug discovery. Curr Pharm Des 2000;6:379–392.
17. Sausville EA, Johnson J, Alley M, Zaharevitz D, Senderowicz AM. Inhibition of CDKs as a therapeutic modality. Ann NY Acad Sci 2000;910:207–221.
18. Tannoch VJ, Hinds PW, Tsai LH. Cell cycle control. Advan in Experim Med and Biol 2000;465:127–140.
19. Morgan D. Cyclin dependent kinases: Engines, clocks and microprocessors. Annu Rev Cell Dev Biol 1997;13:261–291.
20. Malumbres M, Barbacid M. To cycle or not to cycle: A critical decision in cancer. Nat Rev Cancer 2001;1:222–231.

21. Sherr CJ, Roberts JM. CDK inhibitors: Positive and negative regulators of G1-phase progression. Genes Dev 1999; 13:1501–1512.
22. Pavletich NP. Mechanism of cyclin-dependent kinase regulation structures of cdks, their cyclin activators, and CIP and INK4 inhibitors. J Mol Biol 1999;287:821–828.
23. Sandal T. Molecular aspects of the mammalian cell cycle and cancer. Oncologist 2002;7:73–81.
24. Gu Y, Turck CW, Morgan DO. Inhibition of CDK2 activity in vivo by an associated 20K regulatory subunit. Nature 1993;366:707–710.
25. Deiry WS, Tokino T, Velculescu VE. Waf1, a potential mediator of p53 tumor suppression. Cell 1993;75:817–825.
26. Jiang H, Lin J, Su ZZ, Collart FR, Huberman E, Fisher PB. Induction of differentiation in human promyelocitic HL-60 leukemia cells activates p21, WAF/CIP1, expression in the absence of p53. Oncogene 1994;9:3397–3406.
27. Steinman RA, Hoffman B, Iro A, Guillouf C, Lieberman DA, el-Houseini ME. Induction of p21 (WAF/CIP1) during differentiation. Oncogene 1994;9:3389–3396.
28. Gonzales CA. Nutrition and cancer: The current epidemiological evidence. Br J Nutr 2006;96:S42–S45.
29. Messina M, Barnes S. The role of soy products in reducing risk of cancer. J Natl Cancer Inst 1991;83:541–546.
30. Agarwal C, Singh RP, Dhanalakshmi S, et al. Silibilin upregulates the expression of cylin-dependent kinase inhibitors and causes cell cycle arrest and apoptosis in human colon carcinoma HT-29cells. Oncogene 2003;22: 8271–8282.
31. Yu Z, Li W, Liu F. Inhibition of proliferation and induction of apoptosis by genistein in colon cancer HT-29cells. Cancer Lett 2004;215:159–166.
32. Shen G, Xu C, Chen C, Hebbar V, Kong AT. p53-independent G1 cell cycle arrest of human colon carcinoma cells HT-29 by sulforaphane is associated with induction of p21 and inhibition of expression of expression of cyclin D1. Cancer Chemother Pharmacol 2006;57:317–327.
33. Chen J, Qiu X, Wang R, et al. Inhibition of human gastric carcinoma cell growth in vitro and in vivo by cladosporol isolated from the paclitaxel-producing strain *Alternaria alternata* var. monosporus. Biol Pharm Bull 2009;32: 2072–2074.
34. Wang W, Heideman L, Ching CS, Pelling JC, Koehler KJ, Birt DF. Cell-cycle arrest at G2/M and growth inhibition by apigenin in human colon carcinoma cell lines. Mol Carcinog 2000;28:102–110.
35. Matsui TA, Sowa Y, Murata H, et al. The plant alkaloid cryptolepine induces $p21^{waf1/Cip1}$ and cell cycle arrest in a human osteosarcoma cell line. Int J Oncol 2007;31:915–922.
36. Nakano K, Mizuno T, Sowa Y, et al. Butyrate activates the WAF1/CIP1 gene promoter through Sp1 sites in a p53-negative human colon cancer cell line. J Biol Chem 1997; 272:22199–22206.
37. Vascotto C, Cesaratto L, D'Ambrosio C, et al. Proteomic analysis of liver tissues subjected to early ischemia/reperfusion injury during human orthotopic liver transplantation. Proteomics 2006;6:3455–3465.
38. Gartel AL, Tyner AL. Transcriptional regulation of the $p21^{waf1/cip1}$ gene. Exp Cell Res 1999;246:280–289.
39. Han S, Sidell N, Fisher PB, Roman J. Up-regulation of p21 gene expression by peroxisome proliferator-activated receptor γ in human lung carcinoma cells. Clin Cancer Res 2004;10:1911–1919.
40. Hong JK, Samudio I, Liu S, Abdelrahim M, Safe S. Peroxisome proliferator-activated receptor γ-dependent activation of p21 in Panc-28 pancreatic cancer cells involves Sp1 and Sp4 proteins. Endocrinology 2004;145:5774–5785.
41. Bonofiglio D, Qi H, Gabriele S, et al. Peroxisome proliferator-activated receptor γ inhibits follicular and anaplastic thyroid carcinoma cells growth by upregulating $p21^{waf1/cip1}$ gene in a Sp1-dependent manner. Endocrine Relat Cancer 2008;15:545–557.
42. Ong CS, Tran E, Nguyen TT, et al. Quercetin-induced growth inhibition and cell death in nasopharyngeal carcinoma cells are associated with increase in Bad and hypophosphorylated retinoblastoma expressions. Oncol Rep 2004;11:727–733.
43. Agarwal C, Singh RP, Dhanalakshmi S, et al. Silibinin upregulates the expression of cyclin-dependent kinase inhibitors and causes cell cycle arrest and apoptosis in human colon carcinoma HT-29cells. Oncogene 2003;22:8271–8282.
44. Grana X, Reddy P. Cell cycle control in mammalian cells: Role of cyclins, cyclin dependent kinases (CDKs), growth suppressor genes and cyclin-dependent kinase inhibitors (CKIs). Oncogene 1995;11:211–219.
45. Paggi MG, Baldi A, Sonetto F, Giordano A. Retinoblastoma protein family in cell cycle and cancer: A review. J Cell Biochem 1996;62:418–430.
46. Cayrol C, Knibiehler M, Ducommun B. p21 binding to PCNA causes G1 and G2 cell cycle arrest in p53-deficient cells. Oncogene 1998;16:311–320.
47. Biggs JR, Kudlow JE, Kraft AS. The role of the transcription factor Sp1 in regulating the expression of the WAF1/CIP1 gene in U937 leukemic cells. J Biol Chem 1996; 271:901–906.
48. Datto MB, Yu Y, Wang XF. Functional analysis of the transforming growth factor beta responsive elements in the WAF1/Cip1/p21 promoter. J Biol Chem 1995;270: 28623–28628.
49. Lee SJ, Ha MJ, Lee J, et al. Inhibition of the 3-hydroxy-3-methylglutaryl-coenzime A reductase pathway induces p53-independent transcriptional regulation of p21(WAF1/CIP1) in human prostate carcinoma cells. J Biol Chem 1998;273:10618–10623.
50. Sowa Y, Orita T, Minamikawa S, et al. Histone deacetylase inhibitor activates the WAF1/Cip1 gene promoter through the Sp1 sites. Biochem Biophys Res Commun 1997; 241:142–150.
51. Billon N, Carlisi D, Datto MB, van Gruyten LA, Wang XF, Rudkin B. Cooperation of Sp1 and p300 in the induction of the CDK inhibitor p21/WAF1/CIP1 during NGF-mediated neuronal differentiation. Oncogene 1999;6: 2872–2882.
52. Rooversand K, Assoian RK. Integrating the MAP kinase signal into the G1 phase cell cycle machinery. Bioessays 2000;22:818–826.
53. Oh SY, Park KS, Kim JA, Choi KY. Differential modulation of zinc-stimulated p21(Cip/WAF1) and cyclin D1 induction by inhibition of PI3 kinase in HT-29 colorectal cancer cells. Exp Mol Med 2002;34:27–31.